HHS Public Access

Author manuscript

Biochem Biophys Res Commun. Author manuscript; available in PMC 2015 April 27.

Published in final edited form as:

Biochem Biophys Res Commun. 2010 April 30; 395(2): 168–172. doi:10.1016/j.bbrc.2010.03.108.

The Prostaglandin Transporter PGT Transports PGH_2

Yuling Chi[a] and **Victor L. Schuster**[a,b]

[a]Department of Medicine, Division of Nephrology, Albert Einstein College of Medicine, Bronx, NY

[b]Department of Physiology and Biophysics, Albert Einstein College of Medicine, Bronx, NY

Abstract

Prostaglandin H_2 not only serves as the common precursor of all other PGs, but also directly triggers signals (eg. platelet aggregation), depending on its location and translocation. The prostaglandin carrier PGT mediates the transport of several prostanoids, such as PGE_2, and $PGF_{2\alpha}$. Here we used PGT in the plasma membrane as a model system to test the hypothesis that PGT also transports PGH_2. Using wild type and PGT-expressing MDCK cells, we show that PGH_2 uptake is mediated both by simple diffusion and by PGT. The PGH_2 influx permeability coefficient for diffusion is $(5.66 \pm 0.63) \times 10^{-6}$ cm/s. The kinetic parameters of PGH_2 transport by PGT are $K_m = 376 \pm 34$ nM and $V_{max} = 210.2 \pm 11.4$ fmoles/mg protein/s. PGH_2 transport by PGT can be inhibited by excess PGE_2 or by a PGT inhibitor. We conclude that PGT may play a role in transporting PGH_2 across cellular membranes.

Keywords

prostaglandin H_2; prostaglandin transporter

Introduction

Prostaglandin H_2 (PGH_2) is the common precursor of all other PGs (PGE_2, PGI_2, PGD_2 and PGF_2) and thromboxane A_2 (TxA_2). It is converted to these PGs by the specific terminal synthases in the cytoplasm (1-6). Besides serving as a common precursor, extracellular PGH_2 can directly trigger signals including Ca^{2+} release, serotonin release, vasoconstriction, and platelet aggregation (7-10). The signals induced by extracellular PGH_2 can therefore oppose the signals resulting from intracellular PGH_2, such as formation of PGI_2, the most potent endogenous inhibitor of platelet aggregation (11, 12). Thus the net result of PGH_2 depends on its localization of PGH_2. Of interest, Kent et al. (9) reported that endothelial cells exposed to PGH_2 produced PGI_2, suggesting that PGH_2 might be taken up into

Address Correspondence to Victor L. Schuster, Department of Medicine, Albert Einstein College of Medicine, NY 10461; Tel. 718 430-8560; Fax. 718 430-8963; victor.schuster@einstein.yu.edu.

endothelial cells and converted to PGI_2 by PGI_2 synthase. This raises the question of how PGH_2 translocation occurs.

The prostaglandin transporter (PGT) has been shown to transport several prostaglandins, including PGE_2 (13, 14). PGT mediates the active uptake of PGE_2 into the cell against a concentration gradient (15). Based on the structural similarity between PGH_2 and PGE_2, as shown in Fig. 2C and D, we hypothesized that PGT might also transport PGH_2. Using MDCK cells stably expressing PGT, as previously reported (16), we conducted a detailed investigation of the kinetics of PGH_2 transport by PGT. The competition of transport by PGT between PGH_2 and PGE_2, and the inhibition of PGH_2 transport by our newly identified PGT inhibitor, TGBz T34 (15), confirmed that PGH_2 is, indeed, a substrate of PGT.

Materials and methods

MDCK cells were stably transfected with the GFP-tagged PGT in our laboratory (16). Tritium labeled PGE_2 ($[^3H]PGE_2$) and PGH_2 ($[^3H]PGH_2$) were purchased from PerkinElmer and CaymanChem, respectively. Unlabeled PGE_2 was obtained from CaymanChem.

Time Course of PGH_2 or PGE_2 Transport

MDCK cells were seeded at 15-20% confluence on 24-well plates. The day on which the cells were seeded was considered day one. PGE_2 uptake experiments were conducted on day 4. All of the PGH_2 or PGE_2 uptake experiments were conducted at room temperature. On day 4, cells were washed twice with Waymouth buffer (135 mM NaCl, 13 mM H-Hepes, 13 mM Na-Hepes, 2.5 mM $CaCl_2$, 1.2 mM $MgCl_2$, 0.8 mM $MgSO_4$, 5 mM KCl, and 28 mM D-glucose). Then 200 μL of Waymouth buffer containing 1 μM $[^3H]PGH_2$ or 1 nM $[^3H]PGE_2$ were added to each well. At the designated time, the uptake of $[^3H]PGH_2$ or $[^3H]PGE_2$ was stopped by aspiration of uptake buffer, followed immediately by two washes with 500 μL of chilled Waymouth buffer. Cells were then lysed with 100 μL lysis buffer containing 0.25% SDS and 0.05 N NaOH. 1.5 mL of scintillation solution was added to each well, and intracellular $[^3H]PGH_2$ or $[^3H]PGE_2$ was counted by MicroBeta scintillation Counter.

To obtain the time course of PGE_2 transport in the presence of PGH_2 or TGBz T34, MDCK cells were incubated in Waymouth buffer containing 1 nM $[^3H]PGE_2$ at room temperature for 9 minutes to reach the maximum intracellular level. Thereafter, either PGH_2 or TGBz T34 was added to the uptake buffer at a final concentration of 2.5 μM or 25 μM. At the designated time, the uptake of $[^3H]PGE_2$ was stopped and uptake was assessed as described above. For the time course of PGH_2 uptake in the presence of TGBz T34, MDCK cells were incubated in Waymouth buffer containing 1 μM $[^3H]PGH_2$ at room temperature for 120 minutes to reach the maximum intracellular level. At 120 minutes, TGBz T34 was added to the uptake buffer at a final concentration of 25 μM. Then the transport was stopped at varied time points and uptake was quantified as above.

Measurements of Kinetic Parameters of PGE_2 and PGH_2

We repeated the time courses of PGE_2 or PGH_2 uptake in the presence or absence of 25 μM TGBz T34 at various initial extracellular concentrations of PGE_2 (0, 20, 40, 80, 120, 160, and 300 nM) or PGH_2 (0, 10, 25, 50, 100, 250, 500, and 1000 nM). In the case of PGE_2, at

low concentrations, the extracellular concentrations were taken as ^{3}H labeled PGE_2, which has a specific activity of 500 μCi/mol. At high concentrations of PGE_2, we made a mixture of ^{3}H labeled and unlabeled PGE_2 to a final specific activity of 25 μCi/mol.

The initial velocities at various extracellular concentrations of PGE_2 or PGH_2 were determined from the PGE_2 uptake in the first 2 minutes or the PGH_2 uptake in the first 3 minutes, in the presence or absence of TGBz T34; these were linear over the early time course of PGE_2 or PGH_2 uptake. The permeability coefficient of PGH_2 or PGE_2 influx (P_{in}) was obtained by linear regression fit of the initial rate in the presence of TGBz T34 *versus* extracellular PGE_2 or PGH_2 concentration.

We subtracted the initial velocities in the presence of TGBz T34 from those in the absence of TGBz T34. These resulted initial velocities were used to obtain K_m and V_{max} values by nonlinear regression fit of the initial rate *versus* extracellular PGE_2 or PGH_2 concentration to the Michaelis-Menten equation ($V_i = V_{max}[S] / ([S] + K_m)$).

Results

Time Course of PGH_2 Uptake

The time course of PGH_2 uptake by MDCK cells expressing PGT is shown in Fig. 1A. The circles represent the total PGH_2 uptake when the cells were incubated with 1 μM [^{3}H]PGH_2. Squares indicate experiments in which cells were incubated with 1 μM [^{3}H]PGH_2 in the presence of 25 μM TGBz T34, our newly identified PGT inhibitor (15). The line with diamonds represents PGH_2 total uptake minus PGH_2 influx when the PGT inhibitor was applied, which is equivalent to PGT-mediated uptake. The “overshoot” is characteristic of PGT (17).

Fig. 1B shows PGH_2 uptake by wild-type MDCK cells. The inset of Fig. 1B shows the time course of PGH_2 uptake by wild-type MDCK cells for the first 15 minutes. It is evident that PGH_2 influx in PGT-expressing cells plus the inhibitor TGBZ T34 (squares in Fig. 1A) is almost identical to the data of Fig. 1B; each of these represents PGH_2 influx by simple diffusion. Since the pattern of total PGH_2 uptake was similar to that of PGT-mediated uptake, we conclude that PGT mediates the majority of PGH_2 uptake.

Kinetics of PGH_2 Uptake in Comparison with PGE_2 Uptake

To obtain detailed kinetic parameters of PGH_2 influx, we measured initial rates of PGH_2 uptake at various extracellular PGH_2 concentrations in the presence and absence of TGBz T34. In the presence of PGT inhibitor, the plot of the initial rates of PGH_2 uptake versus concentration could be fitted with a straight line (squares in Fig. 2A), indicating that this part of influx was caused by simple diffusion. We calculated the permeability coefficient of PGH_2 influx (P_{in}) by diffusion by dividing the slope of this linear line by the total cell surface. P_{in} for PGH_2 was $(5.66 \pm 0.63) \times 10^{-6}$ (Table 1).

In the absence of TGBZ T34, the plot with circles depicts the total PGH_2 uptake (Fig. 2A). The PGT mediated rates (diamonds) from Fig. 2A were obtained by subtracting the influx by diffusion (squares) from the total influx (circles). When plotted against PGH_2

concentration, they could be fitted by the Michaelis-Menton equation (Fig. 2A). The binding constant of PGH_2 to PGT, K_m, and the maximum velocity, V_{max}, are listed in Table 1. PGT-mediated transport constituted 80% of PGH_2 influx; the remainder was mediated by diffusion.

Using the same method, we conducted a similar investigation of the kinetics of PGE_2 uptake. As shown in Fig. 2B, circles depict the total PGE_2 uptake in the absence of TGBz T34, and squares depict the PGE_2 influx in the presence of TGBz T34. The plot of the latter is linear and shows the component of PGE_2 influx caused by diffusion. P_{in} for PGE_2, was $(1.06 \pm 0.13) \times 10^{-6}$ cm/s (Table 1). Using the same methods as for analyzing PGH_2 kinetics, we generated the PGT-mediated uptake component (diamonds), which could be fitted by the Michaelis-Menton equation. The binding constant of PGE_2 to PGT, K_m, and the maximum velocity, V_{max}, are listed in Table 1. As opposed to the case with PGH_2, PGT-mediated PGE_2 transport was almost identical to total PGE_2 uptake, suggesting that PGE_2 influx is mainly mediated by PGT. Comparison of the kinetic parameters of PGE_2 to PGH_2 uptake shows that P_{in} for PGH_2 was 5-fold that for PGE_2; K_m of PGH_2 was 4.1-fold that of PGE_2; and V_{max} of PGH_2 was 2.7-fold that of PGE_2.

To address the possibility that ^{3}H-PGH_2 was metabolized to ^{3}H-PGE_2 and that the measured tracer influx therefore represented ^{3}H-PGE_2, and not ^{3}H-PGH_2, we added 0, 0.5, or 1.0 μM unlabeled PGH_2 to the medium overlaying WT MDCK cells at 37°C, waited 3 minutes, and determined the resulting PGE_2 concentrations by enzyme-linked immunoassay. The resulting medium PGE_2 concentrations were 0.159 ± 0.014, 0.166 ± 0.014, and 0.156 ± 0.017 n*M* (n = 3), respectively. These trivial levels of PGE_2 are well below the affinity of PGT (Table 1), indicating that conversion of PGH_2 to PGE_2 cannot account for our uptake results.

PGH_2 serves as a PGT anion exchange substrate

In the absence of an extracellular substrate for PGT, PGE_2 efflux occurs exclusively by diffusion (15, 17). However, when a PGT substrate is present in the extracellular medium, PGE_2 efflux is accelerated via PGT acting as an obligate anion exchanger (17). In the following experiments, we examined whether unlabeled extracellular PGH_2, like unlabeled extracellular PGE_2, can serve as a “trans” exchange partner to drive tracer PGE_2 efflux.

As shown in Fig. 3 (circles), under control conditions the cells could be rapidly loaded with ^{3}H-PGE_2 such that intracellular ^{3}H-PGE_2 reached a peak at 9 min and leveled off thereafter. This biphasic pattern results from a “pump-leak” system in which PGT-mediated uptake (“pump”) initially exceeds the diffusion-mediated efflux (“leak”) rate (18). As expected from our prior work (15), application of 25 μM TGBz T34 at 9 minutes abruptly stopped further PGT-mediated ^{3}H-PGE_2 uptake. The subsequent rate of ^{3}HPGE_2 efflux represents the background diffusional leak (dots in Fig. 3).

We repeated the experiment, but this time added 2.5 μM unlabeled extracellular PGH_2 during the ^{3}H-PGE_2 uptake. Intracellular ^{3}H-PGE_2 fell to baseline within 5 minutes and remained at that level for the rest of the time course. Of note, extracellular PGH_2 induced a

faster efflux of intracellular ^{3}H-PGE_2 than TGBz T34, indicating that PGH_2 exchanges with ^{3}H-PGE_2 on PGT.

Diffusional efflux of PGH_2

Because PGH_2 influx can occur to some extent by diffusion (Fig. 2 and Table 1), we examined the degree to which PGH_2 also effluxes from cells by diffusion. Toward this end, we loaded cells via PGT for 120 minutes with ^{3}H- PGH_2 to a peak level, and then stopped further uptake with 25 μM TGBz T34. As shown in Fig. 4, this block of carrier-mediated PGH_2 uptake was followed by a rapid depletion of intracellular ^{3}H-PGH_2.This pattern is qualitatively the same as for PGE_2 (Fig. 3), and indicates that pre-loaded ^{3}H-PGH_2 exits cells by diffusion in the same fashion as pre-loaded PGE_2.

Discussion

PGH_2 serves as the common precursor of all other prostaglandins inside cells. It is also rapidly released into the extracellular compartment (Fig. 3) where it can trigger Ca^{2+} release and platelet aggregation by activating its receptor (7-10, 19). These signals could be reduced as PGH_2 was taken back up into cells and converted into other PGs, including PGI_2, which inhibits platelet aggregation. It appears that PGH_2 plays different roles and may trigger opposing signals, directly or indirectly, from different cellular compartments. Therefore, its translocation is critical for its level in either the intracellular or extracellular compartments. Here, we show that PGH_2 efflux is mainly mediated by diffusion and its influx is mediated by both passive diffusion and by a carrier, PGT.

Compared to PGE_2, PGH_2 is transported by PGT with a lower affinity, but at a higher rate. Using transport across the plasma membrane as a model system, we found that PGH_2 has a higher passive permeability than PGE_2. The time course of PGH_2 uptake across the plasma membrane in our assay system is different from that of PGE_2 uptake (Fig. 1A and 3). It took about two hours for PGH_2 to reach a peak intracellular level, whereas it took only 10 minutes for PGE_2 to do so. This is in spite of the fact that about 20% of PGH_2 influx is caused by diffusion, whereas PGE_2 influx by diffusion is negligible. Correspondingly, the efflux of PGH_2 caused by simple diffusion is much greater than that of PGE_2. Therefore, in the “pump-leak” system of PGT-mediated uptake and diffusional efflux, the latter component is much higher for PGH_2 than for PGE_2.

The differences in transport kinetics between PGH_2 and PGE_2 are likely due to chemical structure differences. PGH_2 has a 7-member ring with two oxygens at the head of the molecule, whereas PGE_2 has a five-member ring with a hydroxyl group. Although there are two oxygens in the 7-membrane ring, PGH_2 is more hydrophobic than PGE_2 because of its lack of a hydroxyl group. This greater hydrophobicity probably accounts for the higher passive diffusion of PGH_2 relative to PGE_2. The same structural difference probably accounts for the weaker binding of PGH_2 to PGT, as compared to PGE_2, implying that it is the head of the fatty acid that is interacting with PGT. The -OH group on the ring of PGE_2 is important for the interaction, and it is likely to be a proton donor instead of an acceptor, in order for PGE_2 to be differentiated from PGH_2.

Although PGH_2 binds to PGT more weakly than PGE_2, the V_{max} of PGH_2 is higher than that of PGE_2, indicating that PGT turns over PGH_2 faster than PGE_2. The V_{max} of PGH_2 is 2.7-fold that of PGE_2. Given the same amount of PGT, k_{cat} of PGH_2 will be 2.7 folds of that of PGE_2. The ratio of K_m of PGH_2 to that of PGE_2 is 4.1. The specificity of PGT for a substrate is defined by k_{cat}/K_m. Since k_{cat}/K_m for PGE_2 is 1.5 fold that for PGH_2, we conclude that PGT slightly prefers PGE_2 over PGH_2.

As shown in Fig. 3B and 4, TGBz T34 exerted full inhibition of PGE_2 transport, implying that almost 100% of PGE_2 influx was mediated by PGT. In the case of PGH_2 uptake, TGBz T34 inhibited 80% of PGH_2 transport, consistent with the conclusion that about 80% of PGH_2 uptake was mediated by PGT and about 20% by diffusion (Fig. 2A and 4).

PGH_2 is synthesized by two enzymes cyclooxygenase (COX)-1 or –2, which have been localized to the luminal surfaces of the endoplasmic reticulum (ER) (20), at specific activities of 25 – 40 nmoles/min/mg protein (21-23). PGH_2 is consumed in the cytoplasm by the prostaglandin synthases (PGDS, PGES, PGFS, PGIS), at specific activities of 1 – 4000 nmoles/min/mg protein (1; 2; 4-6; 24-30). The luminal surface of the ER is topologically similar to the exofacial surface of the plasma membrane. Thus, present studies shed light on the kinetics of PGH_2 transport across the ER membrane. The specific transport activity of PGT for PGH_2 is in the range of 0.012 - 1 nmoles/min/mg protein. If PGH_2 translocation from the ER lumen to the cytoplasm is rate-limiting for prostaglandin synthesis, PGT might control the translocation of PGH_2 across the ER, and therefore the accessibility of PGH_2 to the terminal prostaglandin synthases.

In any event, PGT-mediated uptake of PGH_2 may regulate the net signaling that PGH_2 triggers. PGT is strongly expressed in endothelial cells and its expression is induced when endothelial cells are under sheer stress (31-33). PGH_2-induced platelet aggregation would be counteracted by the anti-coagulation effect of PGI_2, formed after PGH_2 is transported into endothelial cells by PGT.

Acknowledgements

Supported by NIH 2RO-1 DK 49688-12 and NIH P50 DK064236-01

Abbreviations

PG	Prostaglandin
PGT	prostaglandin transporter
PGH_2	prostaglandin H_2
PGE_2	prostaglandin E_2
AA	arachidonic acid
TxA_2	thromboxane A_2
COX	cyclooxygenase
ER	endoplasmic reticulum

References

1. Pinzar E, Miyano M, Kanaoka Y, Urade Y, Hayaishi O. Structural basis of hematopoietic prostaglandin D synthase activity elucidated by site-directed mutagenesis. J. Biol. Chem. 2000; 275:31239–31244. [PubMed: 10871602]
2. Tanioka T, Nakatani Y, Semmyo N, Murakami M, Kudo I. Molecular identification of cytosolic prostaglandin E_2 synthase that is functionally coupled with cyclooxygenase-1 in immediate prostaglandin E_2 biosynthesis. J, Biol, Chem. 2000; 275:32775–32782. [PubMed: 10922363]
3. Murakami M, Naraba H, Tanioka T, Semmyo N, Nakatani Y, Kojima F, Ikeda T, Fueki M, Ueno A, Oh-ishi S, Kudo I. Regulation of prostaglandin E_2 biosynthesis by inducible membrane-associated prostaglandin E_2 synthase that acts in concert with cyclooxygenase-2. J. Biol. Chem. 2000; 275:32783–32792. [PubMed: 10869354]
4. Chen L-Y, Watanabe K, Hayaishi O. Purification and characterization of prostaglandin F synthase from bovine liver. Arch. Biochem. Biophys. 296. 1992:17–26.
5. Watanabe K, Yoshida Y, Shimizu T, Hayaishi O. Enzymatic formation of prostaglandin F2 alpha from prostaglandin H2 and D2. Purification and properties of prostaglandin F synthetase from bovine lung. J Biol Chem. 1985; 260:7035–7041. [PubMed: 3858278]
6. Liou J-Y, Shyue S-K, Tsai M-J, Chung C-L, Chu K-Y, Wu KK. Colocalization of prostacyclin synthase with prostaglandin H synthase-1 (PGHS-1) but not phorbol ester-induced PGHS-2 in cultured endothelial cells. J. Biol. Chem. 2000; 275:15314–15320. [PubMed: 10809766]
7. Morinelli TA, Niewiarowski S, Daniel JL, Smith JB. Receptor-mediated effects of a PGH2 analogue (U 46619) on human platelets. Am. J. Physiol. 1987; 253:H1035–43. [PubMed: 3688248]
8. Mayeux PR, Morton HE, Gillard J, Lord A, Morinelli TA, Boehm A, Mais DE, Halushka PV. The affinities of prostaglandin H2 and thromboxane A2 for their receptor are similar in washed human platelets. Biochem. Biophys. Res. Commun. 1988; 157:733. [PubMed: 2974286]
9. Kent KC, Collins LJ, Schwerin FT, Raychowdhury MK, Ware JA. Identification of functional PGH2/TxA2 receptors on human endothelial cells. Circ. Res. 1993; 72:958–65. [PubMed: 8477529]
10. Vezza R, Mezzasoma AM, Venditti G, Gresele P. Prostaglandin endoperoxides and thromboxane A2 activate the same receptor isoforms in human platelets. Thromb. Haemost. 2002; 87:114–21. [PubMed: 11848439]
11. Moncada S, Vane JR. Pharmacology and endogenous roles of prostaglandin endoperoxides, thromboxane A2, and prostacyclin. Pharmacol. Rev. 1978; 30:293–331. [PubMed: 116251]
12. Born GVR. Aggregation of blood platelets by adenosine diphosphate and its reversal. Nature. 1962; 194:927–929. [PubMed: 13871375]
13. Kanai N, Lu R, Satriano J, Bao Y, Wolkoff AW, Schuster VL. Identification and characterization of a prostaglandin transporter. Science. 1995; 268:866–869. [PubMed: 7754369]
14. Schuster VL. Molecular mechanisms of prostaglandin transport. Ann. Rev. Physiol. 1998; 60:221–242. [PubMed: 9558462]
15. Chi Y, Khersonsky SM, Chang Y-T, Schuster VL. Identification of a new class of prostaglandin transporter inhibitors and characterization of their biological effects on prostaglandin E_2 transport. J. Pharmacol. Exp. Ther. 2006; 316:1346–1350. [PubMed: 16269530]
16. Nomura T, Lu R, Pucci ML, Schuster VL. The two-step model of prostaglandin signal termination: in vitro reconstitution with the prostaglandin transporter and prostaglandin 15 dehydrogenase. Mol. Pharmacol. 2004; 65:973–978. [PubMed: 15044627]
17. Chan BS, Satriano JA, Pucci ML, Schuster VL. Mechanism of prostaglandin E2 transport across the plasma membrane of HeLa cells and Xenopus oocytes expressing the prostaglandin transporter "PGT". J. Biol. Chem. 1998; 273:6689–6697. [PubMed: 9506966]
18. Chan BS, Endo S, Kanai N, Schuster VL. Identification of lactate as a driving force for prostanoid transport by prostaglandin transporter PGT. Am. J. Physiol. Renal. Physiol. 2002; 282:F1097–F1102. [PubMed: 11997326]
19. Halushka PV, Mais DE, Mayeux PR, Morinelli TA. Thromboxane, prostaglandin and leukotriene receptors. Annu. Rev. Pharmacol. Toxicol. 1989; 29:213–239. [PubMed: 2543270]

20. Spencer AG, Woods JW, Arakawa T, Singer II, Smith WL. Subcellular localization of prostaglandin endoperoxide H synthases-1 and -2 by immunoelectron microscopy. J Biol Chem. 1998; 273:9886–9893. [PubMed: 9545330]
21. Smith WL, Garavito RM, DeWitt DL. Prostaglandin endoperoxide H synthases (cyclooxygenases)-1 and -2. J. Biol. Chem. 1996; 271:33157–33160. [PubMed: 8969167]
22. Laneuville O, Breuer DK, Dewitt DL, Hla T, Funk CD, Smith WL. Differential inhibition of human prostaglandin endoperoxide H synthases- 1 and -2 by nonsteroidal anti-inflammatory drugs. J. Pharmacol. Exp. Ther. 1994; 271:927–934. [PubMed: 7965814]
23. Barnett J, Chow J, Ives D, Chiou M, Mackenzie R, Osen E, Nguyen B, Tsing S, Bach C, Freire J, et al. Purification, characterization and selective inhibition of human prostaglandin G/H synthase 1 and 2 expressed in the baculovirus system. BBA. 1994; 1994; 1209:130–139. [PubMed: 7947975]
24. Urade Y, Fujimoto N, Hayaishi O. Purification and characterization of rat brain prostaglandin D synthetase. J. Biol. Chem. 1985; 260:12410–12415. [PubMed: 3930495]
25. Urade Y, Fujimoto N, Ujihara M, Hayaishi O. Biochemical and immunological characterization of rat spleen prostaglandin D synthetase. J Biol Chem. 1987; 262:3820–3825. [PubMed: 3102495]
26. Jakobsson P-J, Thorén S, Morgenstern R, Samuelsson B. Identification of human prostaglandin E synthase: a microsomal, glutathione-dependent, inducible enzyme, constituting a potential novel drug target. PNAS. 1999; 96:7220–7225. [PubMed: 10377395]
27. Watanabe K, Kurihara K, Suzuki T. Purification and characterization of membrane-bound prostaglandin E synthase from bovine heart. BBA. 1999; 1439:406–414. [PubMed: 10446427]
28. Tanikawa N, Ohmiya Y, Ohkubo H, Hashimoto K, Kangawa K, Kojima M, Ito S, Watanabe K. Identification and characterization of a novel type of membrane-associated prostaglandin E synthase. Biochem. Biophys. Res. Commun. 2002; 291:884–889. [PubMed: 11866447]
29. Suzuki T, Fujii Y, Miyano M, Chen L-Y, Takahashi T, Watanabe K. cDNA cloning, expression, and mutagenesis study of liver-type prostaglandin F synthase. J. Biol. Chem. 1999; 274:241–248. [PubMed: 9867836]
30. Hara S, Miyata A, Yokoyama C, Inoue H, rugger RB, Lottspeich F, Ullrich V, Tanabe T. Isolation and molecular cloning of prostacyclin synthase from bovine endothelial cells. J Biol Chem. 1994; 269:19897–19903. [PubMed: 8051072]
31. Bao Y, Pucci ML, Chan BS, Lu R, Ito S, Schuster VL. Prostaglandin transporter PGT is expressed in cell types that synthesize and release prostanoids. Am. J. Physiol. Renal Physiol. 2002; 282:F1103–10. [PubMed: 11997327]
32. Pucci ML, Chakkalakkal B, Liclican EL, Leedom AJ, Schuster VL, Abraham NG. Augmented heme oxygenase-1 induces prostaglandin uptake via the prostaglandin transporter in micro-vascular endothelial cells. Biochem. Biophys. Res. Commun. 2004; 323:1299–1305. [PubMed: 15451438]
33. Ulrich, D.; Ulrich, F.; Silny, J.; Unglaub, F.; Pallua, N. Handchir. Mikrochir. Plast Chir. Vol. 38. German: 2006. [Chiparray-based identification of gene expression in HUVECs treated with low frequency electric fields]; p. 149-155.

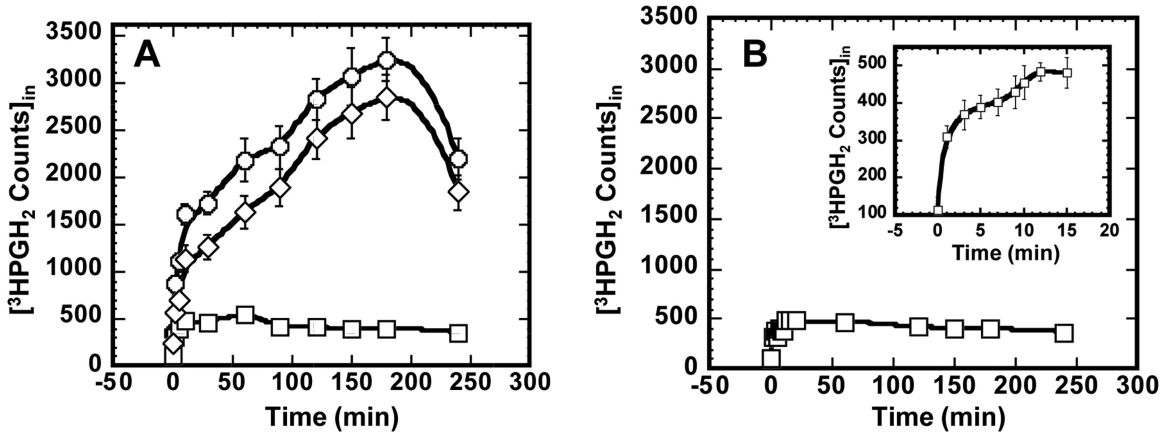

Fig. 1.

A, time course of PGH_2 uptake by PGT-expressing MDCK cells in the presence (squares) and absence (circles) of 25 μM TGBz T34. The diamond line is formed by subtracting intracellular PGH_2 in the absence of TGBz T34 (circles) by intracellular PGH_2 in the presence of TGBz T34 (squares). B, time course of PGH_2 uptake by wild type MDCK cells. In both A and B, the values are presented as mean ± S.D. of three individual replicates.

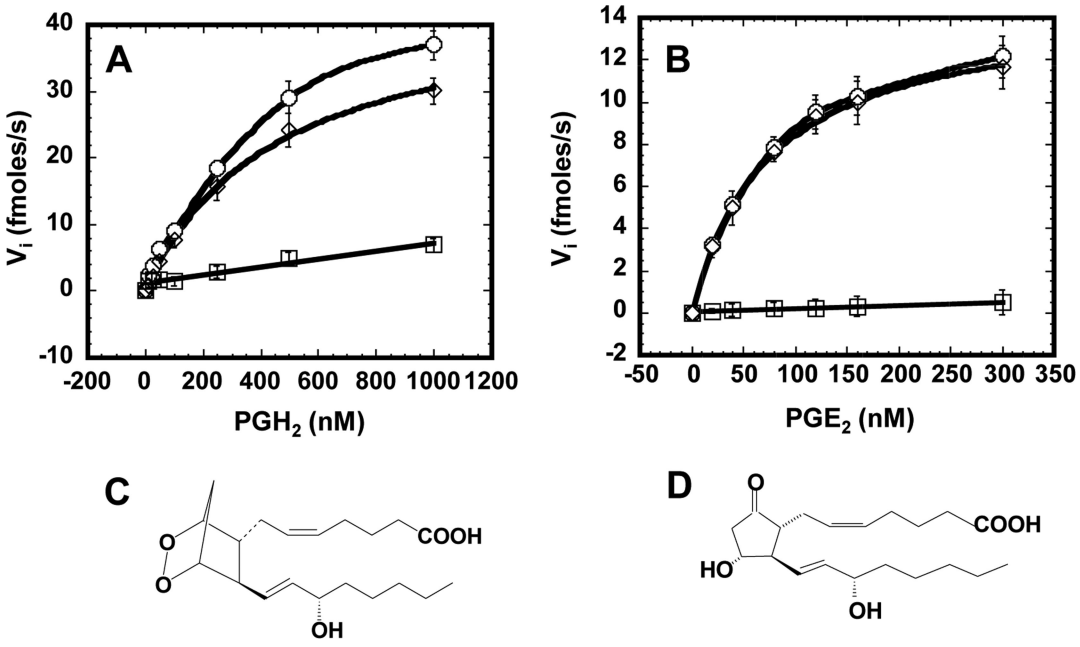

Fig. 2.

Plots of initial velocity of PGH_2 (A) or PGE_2 (B) uptake by PGT-expressing MDCK cells in the presence (squares) or absence (circles) of 25 μM TGBz T34 as a function of PGH_2 (A) or PGE_2 (B) concentration. Circles represent the total uptake and squares represent diffusional influx. The diamonds, which represent [total - diffusional] could be fit by the Michaelis-Menton equation ($V_i = V_{max}$ [S] / ([S] + K_m)). These are representative plots of three individual sets of experiments. In each set of experiment, the error bars are S.D. values of triplicates. The kinetic parameters were generated in each of 3 sets of experiments and presented as mean values ± S.D. in Table 1. C and D, chemical structures of PGE_2 and PGH_2, respectively

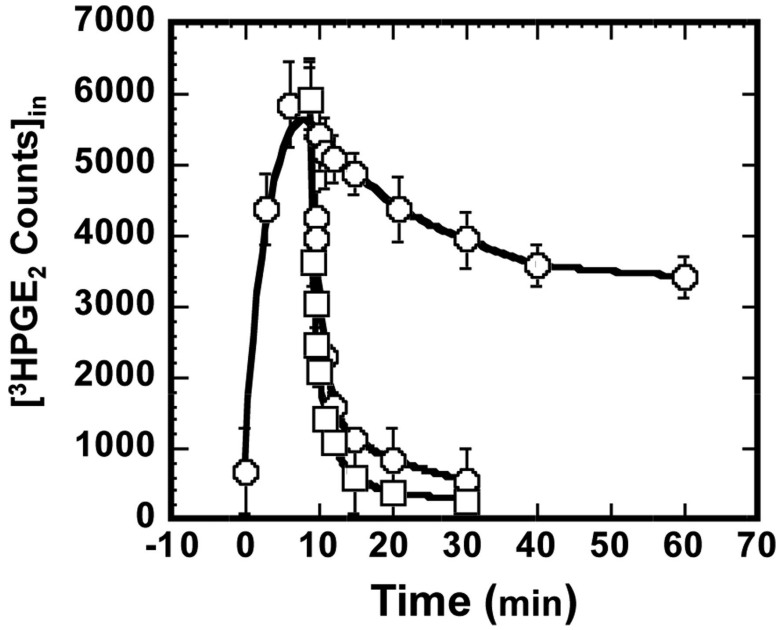

Fig. 3.

Time Course of PGE_2 uptake by PGT-expressing MDCK cells in the absence (circles) and presence of 2.5 μM PGH_2 (squares) or 25 μM TGBZ T34 (closed circles). PGE_2 uptake as a function of time was first established by allowing uptake to various time points, washing, and counting intracellular PGE_2 (open circles). In separate experiments, either 2.5 μM PGH_2 or 25 μM TGBZ T34 was added at 10 minutes when intracellular PGE_2 had reached the peak level. Thereafter, PGE_2 uptake was stopped at various points by washing and intracellular PGE_2 was measured. The values are presented as mean ± S.D. of triplicates.

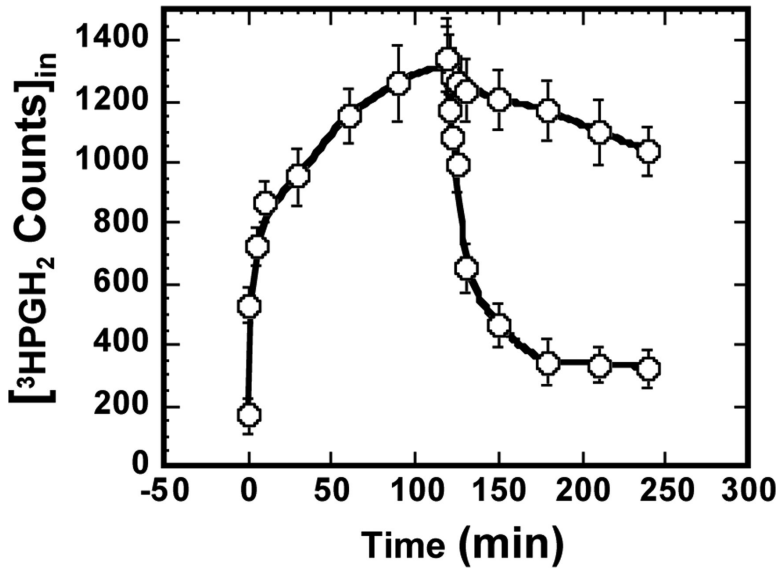

Fig. 4.

Diffusional efflux of PGH_2. As a baseline, ^{3}H-PGH_2 uptake was allowed to proceed to various time points and stopped by washing, and then intracellular ^{3}H-PGH_2 was measured (open circles). In separate experiments, 25 μM TGBZ T34 was added at 120 minutes when intracellular PGH_2 had reached peak level. Thereafter PGH_2 uptake was stopped at various time points by washing and intracellular PGH_2 was measured (closed circles). The values are presented as mean ± S.D. of triplicates.

Table 1

Kinetic parameters of PGH2 and PGE2 influx by both PGT and diffusion.

Kinetic Parameters	**PGH_2**	**PGE_2**
K_m (nM)	376 ± 34	91.0 ± 8.2
V_{max} (fmoles/mg protein/s)	210.2 ± 11.4	78.9 ± 6.9
Influx permeability coefficient (P_{in}) (cm/s)	$(5.66 \pm 0.63) \times 10^{-6}$	$(1.06 \pm 0.13) \times 10^{-6}$

All kinetic parameters are presented as mean ± S.D. (n = 3).